# 8

# IONIC CHANNELS

In the previous chapters, we studied the spread of the membrane potential in passive or active neuronal structures and the interaction among two or more synaptic inputs. We have yet to give a full account of *ionic channels*, the elementary units underlying all of this dizzying variety of electrical signaling both within and between neurons. Ionic channels are individual proteins anchored within the bilipid membrane of neurons, glia, or other cells, and can be thought of as water-filled macromolecular pores that are permeable to particular ions. They can be exquisitely voltage sensitive, as the fast sodium channel responsible for the sodium spike in the squid giant axon, or they can be relatively independent of voltage but dependent on the binding of some neurotransmitter, as is the case for most synaptic receptors, such as the acetylcholine receptor at the vertebrate neuromuscular junction or the AMPA and GABA synaptic receptors mediating excitation and inhibition in the central nervous system. Ionic channels are ubiquitous and provide the substratum for all biophysical phenomena underlying information processing, including mediating synaptic transmission, determining the membrane voltage, supporting action potential initiation and propagation, and, ultimately, linking changes in the membrane potential to effective output, such as the secretion of a neurotransmitter or hormone or the contraction of a muscle fiber.

Individual ionic channels are amazingly specific. A typical potassium channel can distinguish a $K^+$ ion with a 1.33 Å radius from a $Na^+$ ion of 0.95 Å radius, selecting the former over the latter by a factor of 10,000. This single protein can do this selection at a rate of up to 100 million ions each second (Doyle et al., 1998).

At the time of Hodgkin and Huxley's seminal study in the early 1950s, two broad classes of transport mechanisms were competing as plausible ways for carrying ionic fluxes across the membrane: *carrier molecules* and *pores*. At the time, no direct evidence for either one existed. It was not until the early 1970s that the fast ACh synaptic receptor and the Na channel were chemically isolated and purified and identified as proteins. One reason ionic channels were difficult to detect was the tiny amount of current they carry. In a technical breakthrough, Neher and Sakmann (1976) at the Max Planck Institute in Göttingen, Germany, reported the first direct measurement of the electrical current flowing through a single ionic channel using the *patch-clamp* technique. This method, subsequently developed into the *tight* or *giga-seal* recording technique (described in detail in Sakmann and Neher, 1983), allows one to record from very small patches of membrane containing one or a few ionic channels,

using a glass pipette tightly sealed against the neuronal membrane. With modern amplifiers, this recording technology is limited by Johnson thermal noise and can measure currents in the 0.1 pA range. In recognition of the rapid progress in understanding ionic channels and their fundamental role in cellular and neurobiology, Neher and Sakmann were awarded the Nobel prize in Medicine in 1991.

The second technology that has allowed access to the detailed molecular structure of ionic channels is recombinant DNA and the associated instrumentarium of molecular biology. Channels are now routinely cloned, and the effect of replacing individual amino acids on the function of the channel can be assessed. This has allowed scientists to understand the family relationships between different ionic channels. Combined with crystallographic analyses, this has lead to an explosion of studies within the last decade that have characterized the nature of ionic channels, their three-dimensional structure and their biophysical properties, as well as their associated amino acid sequences.

Because of the tiny electrical current carried by individual ionic channels, it can be argued that there is no need to understand their properties in a monograph dedicated to studying macroscopic currents and how these currents underlie information processing. Yet we clearly need to discern the relationship between the macroscopic currents that are responsible for triggering action potentials and initiating synaptic transmission and the microscopic ionic fluxes through channels that underlie them. Different from digital computers, where the engineer strives to isolate the function of the system from its detailed physical properties (e.g., the function of core magnetic memory, bubble memory, CD-ROM, or optical memory is to store bits in certain patterns, regardless of the physical substrate), no such convenient isolation exists in biological systems. Here, *structure reflects function*. Thus, it behooves us to understand the components responsible for electrical signaling.

In the next section, we summarize some of the pertinent properties of ionic channels. We will be brief here; for *the* classical account of the biophysics of ionic channels see Hille (1992); for a more molecular treatment, see Hall (1992). In the section that follows, we introduce the reader to kinetic models of ionic channels. In the third and most important section of this chapter, we detail how microscopic, stochastic channels give rise to macroscopic, deterministic currents, and we provide a justification for why, in this book, we deal exclusively with the latter.

## 8.1 Properties of Ionic Channels

A trace of the tiny electrical current flowing through a single ionic channel as a function of time immediately reveals some of the unique aspects of channels. In the record shown in Fig. 8.1, acetylcholine (ACh) is applied to a single, fast nicotinic channel while the membrane potential across the channel is clamped to −80 mV. Thousands of these channels make up the much-studied neuromuscular endplate, the giant synapse transmitting the output of motoneurons to the muscle. Although the input is constant, the ionic current switches among two states, one defined by zero and the other by 3 nA current flow. These fluctuations are probabilistic in character, with the channel randomly alternating between the opened and the closed state. For ligand-gated synaptic ionic channels, the rates of opening and closing vary when one or more neurotransmitter molecules bind with the channel complex. For voltage-dependent channels, the opening and closing rates vary systematically with the applied membrane potential.

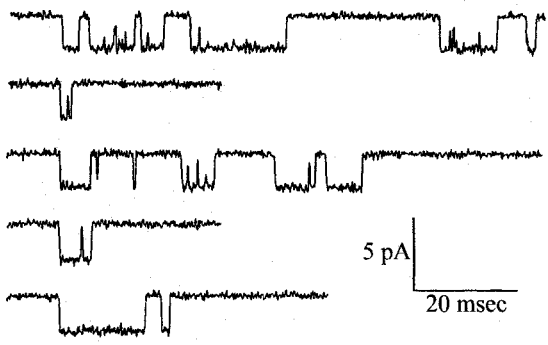


**Fig. 8.1 CURRENT FLOWING THROUGH A SINGLE IONIC CHANNEL** Several excerpts from a patch-clamp recording of a single acetylcholine-activated channel on a cultured muscle cell. The patch was held at a constant membrane potential of −80 mV. The openings of the channel (downward events) cause a unitary 3-nA current to flow, occasionally interrupted by a brief closing. These closings sometimes fail to reach the baseline due to the limited temporal resolution of the apparatus. Notice the random openings and closings of the channel, characteristic of all ionic channels. Fluctuations in the baseline current are due to thermal noise. Reprinted in modified form by permission from Sigworth (1983).

### *8.1.1 Biophysics of Channels*

The single channel whose behavior is observed in Fig. 8.1 appears to act as a binary switching element: either the channel is closed and no current flows or the channel is open and—for a constant applied voltage level—a fixed amount of current flows. As the effective voltage gradient across a voltage-dependent channel is increased, two things change: the probability of opening as well as the amplitude of the current flowing through the channel in its open phase vary. As detailed in Sec. 9.1.1, the current across the membrane is frequently described using a nonlinear model, the Goldman-Hodgkin-Katz constant field equation (Eq. 9.1), as well as Ohm's law. If the Nernst reversal potential of the channel is properly taken into account, Ohm's law appears adequate for many channel types, in particular those permeable to $Cl^-$, $Na^+$, or $K^+$. In other words, the ionic current flowing through a single channel in the open state is given by

$$I_{\text{ionic}} = \gamma(V_m - E_{\text{ionic}}) \tag{8.1}$$

with each channel having a characteristic *unitary channel* conductance $\gamma$ (Fig. 8.2). This value ranges around 10 pS for the fast sodium channels in the squid axon to the very large calcium-dependent potassium channels in mammals with $\gamma \approx 200$–$300$ pS (see Table 8.1).[1]

Upon closer inspection, the $I$–$V$ relationship of the calcium-dependent potassium channel in Fig. 8.2B is not really linear: for large de- or hyperpolarizing voltage excursions, the current through the channel starts to *saturate*. A number of factors are responsible for this. When the concentration gradient between inside and outside is very steep, current passes more easily in one direction than in the other (*rectification*). This is particularly true for calcium channels, with their five orders of magnitude concentration differential across the membrane. A second source of nonlinearities are ions in the intra- or extracellular cytoplasm that move into the channel and block it. Indeed, this is the reason for the nonlinearity of the

1. The value of $\gamma$ depends weakly on temperature, with $Q_{10} \approx 1.3$–$1.6$.

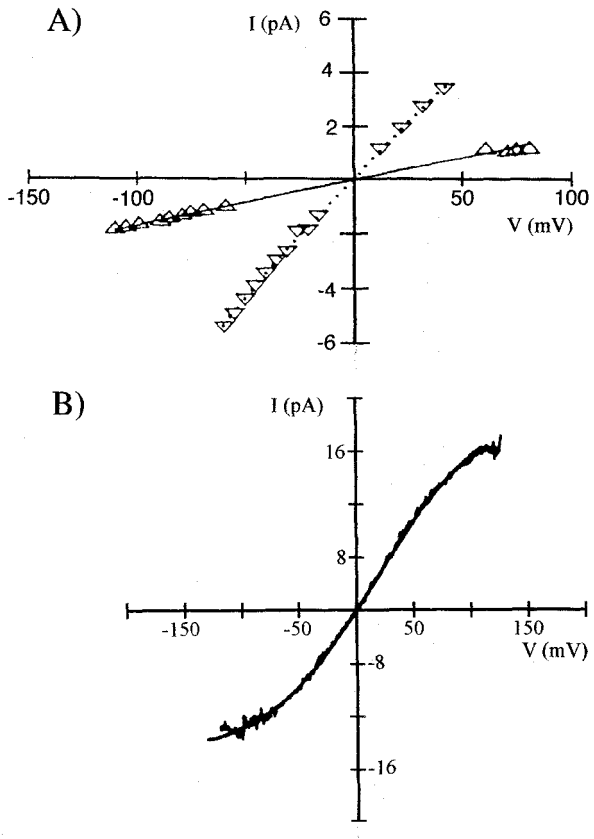


**Fig. 8.2 VOLTAGE DEPENDENCY OF IONIC CHANNELS** **(A)** Current-voltage relationship of a single nicotinic ACh-activated ionic channel. Since the concentration of the permeant ion on both sides of the membrane is identical (here set to either 150 m*M* $NH_4^+$ (downward pointing arrowhead) or $Li^+$ (upward pointing arrowhead)), the reversal potential is zero. As the voltage gradient across the channel increases, so does the current through the channel (up to a limit), in accordance with Ohm's law. The single-channel conductance $\gamma$ is either 17 pS (in $Li^+$) or 79 pS (in $NH_4^+$). Reprinted in modified form by permission from Dani (1989). **(B)** *I–V* relationship for a single voltage- and calcium-dependent potassium channel in a symmetrical 160-mM potassium solution. The slope of this curve around the origin is 265 pS. Deviations from Ohm's law are apparent for large voltage gradients. Reprinted in modified form by permission from Yellen (1984).

NMDA channel (Fig. 4.9A). Another difficulty is that many channels show subconductance levels; that is, they have two or more conductive states, each with its own characteristic conductance and with random voltage-dependent transitions among these sublevels. Indeed, in the long time series from which Fig. 8.1 was excerpted, occasionally the channel opens to a 4.3 pA level (Sigworth, 1983). Many, if not all, channels show evidence of some sublevels; this appears to be particularly true for GABA and glycine channels (Bormann, Hamill, and Sakmann, 1987). Yet another complication is that the current through an open channel sometimes briefly and transiently goes to zero. This rapid closing and opening of the channel is called *flickering* and is thought to be caused by the transient blocking of the pore by some ion or molecule. In some cases this happens so frequently that the current record has the appearance of a comb rather than a rectangular pulse. If the flickering is

**TABLE 8.1**
**Properties of Different Types of Ionic Channels**

| Channel type | Preparation | $\gamma$ | $\eta$ |
|---|---|---|---|
| Fast $Na^+$ | Squid giant axon[1] | 14 | 330 |
| Fast $Na^+$ | Rat axonal node of Ranvier[2] | 14.5 | 700 |
| Fast $Na^+$ | Pyramidal cell body[3] | 14.5 | 4–5 |
| Delayed rectifier $K^+$ | Squid giant axon[4] | 20 | 18 |
| $Ca^{2+}$-dependent $K^+$ | Mammalian preparation[5] | 130–240 | — |
| Transient A current | Insect, snail, mammal[5] | 5–23 | — |
| Nicotinic ACh receptor | Mammalian motor endplate[7] | 20–40 | 10,000 |
| $GABA_A$ $Cl^-$ receptor | Hippocampal granule cells[8] | 14, 23 | — |

Single channel conductance $\gamma$ (in pS) and average channel density $\eta$ if known (per $\mu m^2$) for some ionic channels. The exact value of $\gamma$ depends on many variables, in particular the temperature and the composition of the extracellular fluid.
[1] In the absence of external divalent ions at 5° C; Bezanilla (1987).
[2] At 20° C; Neumcke and Stämpfli (1982).
[3] Hippocampal pyramidal cell body and initial segment at 24° C; Colbert and Johnston (1996).
[4] Between 13–25° C; less frequent are channels with $\gamma = 10$ and 40 nS; Llano, Webb, and Bezanilla (1988).
[5] At 22° C; Latorre and Miller (1983).
[6] At 22° C; Adams and Nonner (1989).
[7] Peak density; the density decreases with distance from active zone; for a review, see Hille (1992).
[8] At 22° C; Edwards, Konnerth, and Sakmann (1990).

too rapid to be adequately resolved by the recording apparatus, it effectively lowers the apparent conductance of the channel. Nevertheless, to a good first approximation one can treat ionic channels as conductances (with the appropriate reversal potential depending on the concentration gradient across the membrane; see Eq. 4.2 and Fig. 8.2A; for more details, see Hille, 1992).[2]

Estimates of the single-channel conductance $\gamma$ based on Ohm's macroscopic law and the geometry of the pore put the upper limit at about 300 pS and no channel with larger conductance has been reported. The current through single channels is usually larger than 1 pA, corresponding to about 6000 monovalent ions passing through the channel each millisecond; indeed most pass more current, with the record somewhere around 27 pA. The diffusion equation places an upper limit of around $10^8$ ions per second diffusing through these small pores, whose width is only one or two atomic diameters at the most restricted part of the channel (Hille, 1992; Doyle et al., 1998).

The density of these channels can vary widely depending on the exact preparation used (Table 8.1). In the squid axon, there are on the order of 300 sodium and 18 potassium channels per square micrometer. Similar numbers hold for other rapidly conducting systems without myelin insulation. In the frog or the rat node of Ranvier, a membrane specialization in myelinated axons where all the sodium channels appear to be concentrated (Sec. 6.6), the density of Na channels can be as high as 2000 per square micrometer. Even at these densities, channel proteins do not constitute major chemical components of most neuronal membranes. In principle, between two and four orders of magnitude additional channels could be packed into the membrane before the maximum molecular crowding sustainable by a membrane is achieved (Hille, 1992). Given ionic fluxes of between $10^7$ and $10^8$ ions per second per channel and a membrane capacitance of around 1 $\mu F/cm^2$, these densities

2. Modern patch-clamp amplifiers have such high resolution that they are limited by the thermal noise of the recorded system, rather than by instrument noise. As is evident in Fig. 8.1, the current measurements fluctuate in both opened and closed states. The standard deviation of these fluctuations—dictated by statistical physics—is typically less than 0.1 pA.

are more than sufficient to lead to the rapid and pronounced changes in membrane potential evidenced in action potential initiation and propagation and other electrical events.

It should be emphasized that the properties of ionic channels discussed here, in particular their microscopic, all-or-none and stochastic nature, hold true regardless of whether we are dealing with ligand-gated NMDA or GABA receptors, voltage-dependent sodium, calcium, or potassium channels or ionic channels in nonneuronal systems, such as in T lymphocytes, cardiac pacemaker cells, muscle cells, mechanosensitive calcium channels in vertebrate hair cells or channels in the unicellular organism *Paramecium*. Furthermore, there appears to be very little systematic difference between channels recorded from molluscs, flies, squids, or mammals. All these channels are to a good, first approximation activated by the same stimuli, respond with the same kinetics, and are blocked by the same agents. In particular, ionic channels in more highly developed animals, such as vertebrates, are no more complex than channels in less complex animals, such as molluscs. Evidence from molecular cloning studies suggests that the major channel families evolved into their present form with the appearance of multicellular organisms about 700 million years ago (Hille, 1992). If these speculations concerning the evolution of channels bear out, nature seems to have converged on a small number of basic circuit elements—aqueous pores built using protein technology—a long time ago and has remained faithful to this basic design across all species.

### 8.1.2 Molecular Structure of Channels

Figure 8.3A shows an electron-microscopic image of an actual ACh-gated channel within its natural habitat, while Fig. 8.3B summarizes in a graphic manner the current working hypothesis for the structure of a voltage-dependent ionic channel. The entire macromolecule

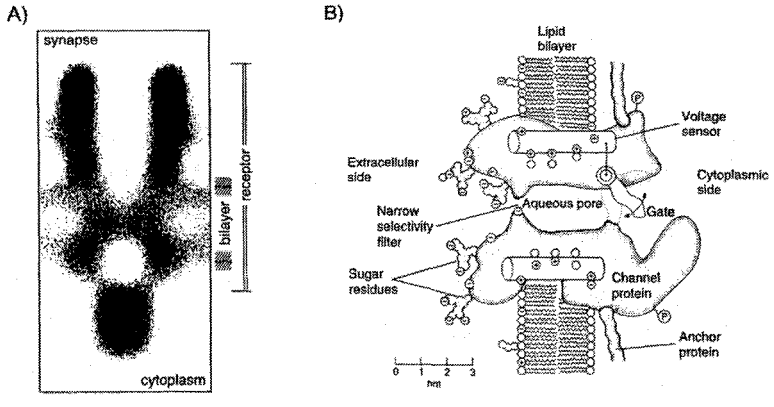


**Fig. 8.3 Molecular Structure of an Ionic Channel** **(A)** Electron-microscopic image using crystallographic methods of the axial section of one of the nicotinic acetylcholine receptors in the electric fish *Torpedo*. This channel has the shape of a tall hour glass, with an overall length of 110 Å. Most of the protein lies outside the bilipid membrane. The complex extends about 20 Å into the cytoplasmic medium and about 60 Å into the extracellular environment. The most narrow portion of the channel is about 8 Å wide. The blob at the bottom of the image is not part of the channel. Reprinted by permission from Toyoshima and Unwin (1988). **(B)** Schematic view of a generic voltage-dependent ionic channel. The molecular details of such channels are now being charted by structural studies (e.g. Doyle et al., 1998). Reprinted by permission from Hille (1992).

making up the channel is sitting in the lipid bilayer of the membrane, anchored to elements of the intracellular cytoskeleton. It is quite large, consisting of several thousand amino acids (and associated sugar residues), with a molecular weight in excess of 300,000 daltons. When the channel is open, it forms a water-filled pore extending across the membrane. The selectivity for certain ions, that is, the fact that the sodium channel is primarily permeable to $Na^+$ ions and not to $K^+$ ions, is conveyed to the channel by the most narrow portion of the channel (termed the *selectivity filter*) with a diameter of around 3 Å(Hille, 1973).

The voltage-dependent gating of the channel is achieved by a conformational change in the three-dimensional shape of part of the molecule, such that the channel is either open or blocked. As discussed already by Hodgkin and Huxley (1952d), this requires the movement of hypothetical *gating particles* able to sense the electric field across the membrane. In fact, at a resting potential of −80 mV an electric field of about 200,000 V/cm is set up across the 40 Åthin membrane. Changes in this field move these gating charges through the membrane and change the configuration of the channel. The steepness of the voltage dependency of the sodium channel (that is, the steepness of $m_\infty^3$ in Sec. 6.2.2) yields an estimate of six elementary gating charges that need to move across the entire membrane in order for a single sodium channel to open. This *gating current*, caused by the channel changing its configuration so that it can conduct current, is tiny compared to the $10^7$ or so ions moving through the open channel each second but has been measured (Armstrong and Bezanilla, 1973). Qualitatively, the gating current can be thought of as a nonlinear capacitive current, proportional to $Q_m dm/dt$, where $Q_m$ is the total charge associated with the transition of the $m$ particle from close to open.

Recombinant DNA technology—in parallel with classical methods such as protein chemistry, X-ray diffraction, and electron microscopy—has given us the opportunity to image channels as well as to derive their amino acid sequence and to clone, express, and manipulate them. (For overviews of this very active research area see Catterall, 1995, 1996 and Doyle et al., 1998.) These methods have allowed the activation and inactivation processes of the sodium channel to be characterized at the molecular level.

The key culprit in voltage-dependent activation are four homologous segments (termed S4) of the sodium channel protein that span the membrane in an $\alpha$ helix. These S4 regions are highly conserved between $Na^+$ channels from different species and are also homologous to specific regions of the voltage-dependent $K^+$ and $Ca^{2+}$ channels. Even before the molecular sequence of these channels was known, Armstrong proposed that two helices, one bearing multiple positive charges and the other multiple negative charges, move relative to each other, perhaps by rotating, so that relative translation by one turn would be equivalent to moving one charge across the membrane. Subsequently, Catterall (1988, 1992) outlined the *sliding helix* model for the action of each S4 segment in activating the channel, a model for which much experimental support is now available (Fig. 8.4). Upon membrane depolarization, each S4 segment rotates by 60°, moving outward by 5 Å. Every third amino acid residue making up this helix is positively charged and is about 5 Å away from the next charged residue. In other words, the rotating movement of the helix effectively moves one charge across the membrane. All four S4 segments, acting in concert, cause the conformational change that leads to the opening of the channel. A similar mechanism, acting also via S4, is thought to confer voltage-dependency onto certain potassium channels (Larsson et al., 1996).

Inactivation is thought to arise by a different process, usually explained by invoking a mechanistic analogy, the *ball-and-chain* model (Armstrong and Bezanilla, 1977; Hoshi, Zagotta, and Aldrich, 1990). Here, a part of the channel molecule on the inner, cytoplasmic

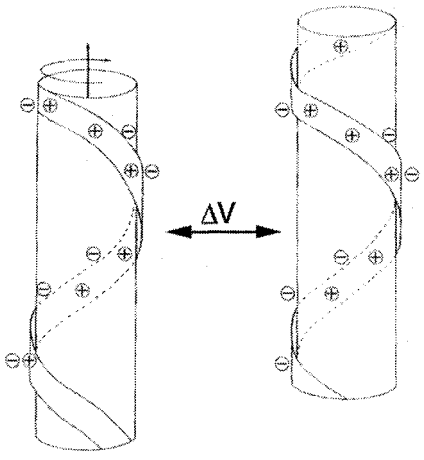


**Fig. 8.4 VOLTAGE-DEPENDENT ACTIVATION OF THE $Na^+$ CHANNEL** *Sliding helix* model postulated by Catterall (1988, 1992) to account for the voltage dependency of activation of the fast sodium conductance underlying action potential generation. The S4 segment of the channel protein that is extended as an $\alpha$ helix throughout the membrane is electrically neutral at rest. In the presence of sufficient depolarization, the helix rotates by 60° in a screw-like outward movement, until it moves into a new stable position, where locally the charges are balanced. The movements of four such S4 segments that are part of the channel molecule are thought to induce a conformational change that leaves the channel in its open state. Reprinted by permission from Catterall (1992).

side of the membrane is thought to act like a tethered gate. Under the right conditions, it swings shut, physically occluding the pore. Zagotta, Hoshi, and Aldrich (1990) showed in a series of elegant site-directed mutagenesis experiments that deletion of the appropriate cytoplasmic part of the inactivating, transient A-type $K^+$ channel molecule does, indeed, eliminate, or greatly reduce, inactivation. Furthermore, if this cytoplasmic region was added as a synthetic soluble peptide, inactivation was restored.

Because of the existence of four S4 segments in the $Na^+$ channel, it can be argued that a better model of sodium current activation would be $m^4$, rather than the $m^3$ term favored by Hodgkin and Huxley (see Eq. 6.13). Yet it needs to be remembered that the Hodgkin–Huxley equations are purely phenomenological fits of the data; the cubic $m$ expression was introduced in order to make a first-order differential equation account for the sigmoidal rise of $I_{Na}$.

Once the detailed molecular structure of the sodium and other channels is worked out, we will be in a better position to derive the relevant equation relating the voltage across the channel to the time-varying current through it. It remains unclear, though, whether more complex models will increase our qualitative understanding of the dynamics of the macroscopic current.

One last comment on the molecular nature of ionic channels. These proteins are so amazingly specific that substituting one amino acid at one of two positions in the several thousands long amino acid sequence coding for the sodium channel with another amino acid will alter the ion-selection properties of the sodium channel to resemble those of calcium channels (Heinemann et al., 1992).

## 8.2 Kinetic Model of the Sodium Channel

In Chap. 6, we saw that Hodgkin and Huxley postulated a number of fictive "gating particles" to satisfactorily describe their macroscopic current records. For any current to flow, several (four in the case of $I_{Na}$) such particles have to come together simultaneously. Given the evidence alluded to above concerning internal repeats in the channel protein, $m$ and $h$ can be reinterpreted in molecular terms as the conformation of these internal repeats (Fig. 8.4). Similar activation and inactivation variables have been postulated for the myriads of sodium,

potassium, calcium, and chloride channels described over the last two decades (see the following chapter).

*Classical kinetic theory* specifies the manner in which one can go from a description of these particles and their underlying states to the final, overall gating scheme. Two key assumptions underlie classical kinetic theory: (1) Gating is a *Markov process*, implying that the rate constants, regulating the transitions from one state to the next, do not depend on the previous history of the system. A sufficient description of the system is its present state, without knowing its previous state. (2) All transitions are assumed to be characterized by a first-order differential equation, with a single associated time constant. The applications of these methods to probabilistic ionic channels are summarized by Neher and Stevens (1977), Colquhoun and Hawkes (1981) and DeFelice (1981).

These two simplifying assumptions are used to construct the overall state diagram of the system, as well as its dynamic behavior, as we will now do for the fast sodium channel. Figure 8.5 illustrates the simplest symmetrical eight-state model of this channel. Here three identical $m$ particles can be either in an "open" or in a "closed" position. $\alpha_m$ can be thought of as proportional to the probability for an $m$ particle to make the transition from closed to open (and $\beta_m$ proportional to the probability for the opposite transition). The fourth $h$ particle can be either in an "inactivated" (top row of Fig. 8.5) or in a "not inactivated" (bottom row) position, with $\alpha_h$ the probability that the $h$ particle will switch from inactivated to open. Alternatively, $m$ can represent the fraction of $m$ gates in their open state and $h$ the fraction of $h$ gates in their noninactivating state. Now, the $\alpha$'s and $\beta$'s need to be interpreted as *rate constants*, governing the rate transitions from one state to the other.

If we assume that the system is in a state where no particle is in its open position, any one of the three identical $m$ particles can open. Since any of these three particles can open, the rate constant is $3\alpha_m$ if we assume that the $m$ particles act independent of each other. For this one open particle to switch back to its closed position, the rate constant is $\beta_m$. To make the next transition from one to two open particles, any one of the two remaining closed particles can switch and the appropriate rate constant is $2\alpha_m$, and so on. For the system to be in its

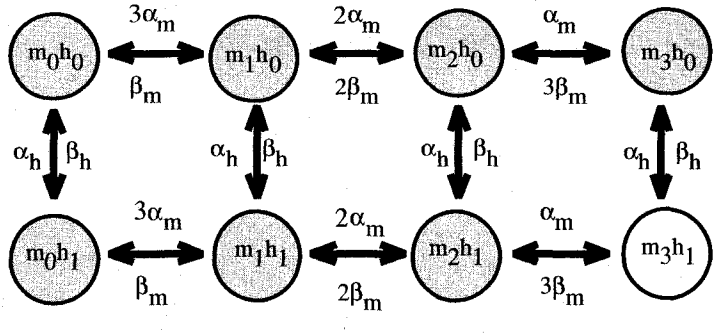


**Fig. 8.5 KINETIC DIAGRAM OF THE FAST SODIUM CHANNEL** Simplest kinetic diagram associated with the fast voltage-dependent $Na^+$ channel. In order for the channel to be in its conductive state, all three $m$ particles as well as the inactivating $h$ particle need to be in their open position. Because we here assume that all three $m$ particles are identical, eight different states exist. $\alpha_m$ is the rate constant at which the $m$ particles switch from their closed to their open positions (that is, moving toward the right in this diagram), while $\beta_m$ is the rate constant for the reverse operation (transition toward the left). Similarly, $\alpha_h$ is the rate constant governing the transition from inactivating to noninactivating state (downward) and $\beta_h$ for the reverse operation. Many more complex gating schemes have been discussed in the literature.

conductive state, the $h$ particle has to switch into the appropriate configuration; thus, of the eight possible different states (from zero $m$ particles open and $h$ closed to all three $m$ as well as $h$ open), only a single one—in the lower right corner in Fig. 8.5—corresponds to the open state.

Assuming the Markov property and first-order transitions among states, leads us to the calculus used by Hodgkin and Huxley in 1952. Following the logic laid out in Chap. 6, if the membrane potential is stepped from its initial value $V_0$ to $V_1$, the fraction of $m$ particles in their activated state follows a simple exponential law,

$$m(t) = m_\infty(V_1) - (m_\infty(V_1) - m_\infty(V_0))e^{-t/\tau_m(V_1)} \tag{8.2}$$

with $m_\infty(V) = \alpha_m(V)/(\alpha_m(V) + \beta_m(V))$ and $\tau_m(V) = 1/(\alpha_m(V) + \beta_m(V))$. With our usual assumption of independence of the gating particles, the fraction of channels populating the conductive $m_3h_1$ state is

$$\begin{aligned} m^3h = &\left(m_\infty(V_1) - (m_\infty(V_1) - m_\infty(V_0))e^{-t/\tau_m(V_1)}\right)^3 \\ &\times \left(h_\infty(V_1) - (h_\infty(V_1) - h_\infty(V_0))e^{-t/\tau_h(V_1)}\right) \end{aligned} \tag{8.3}$$

By multiplying out the exponentials, this equation can be expressed as a sum of seven exponentially decaying terms,

$$m^3h = C_0 + \sum_{i=1}^{7} C_i e^{-t/\tau_i} \tag{8.4}$$

with seven associated time constants $\tau_i = \tau_m$, $2\tau_m$, $3\tau_m$, $\tau_h$, $\tau_m\tau_h/(\tau_m+\tau_h)$, $\tau_m\tau_h/(\tau_m+2\tau_h)$, and $\tau_m\tau_h/(\tau_m + 3\tau_h)$. For a system with eight independent states and first-order transitions among these, seven time constants are expected.

Experimentally, most of these time constants are difficult to resolve, since only the total channel current can be recorded, making the identification of these states difficult. If the three $m$ subunits are assumed to differ from each other in some minor ways, the $Na^+$ channel needs to be characterized by 15 closed and a single open state and by 15 time constants, further compounding the problem. The rate constants between the different states can also be more complex than in the simple scheme illustrated in Fig. 8.5. If *cooperativity* exists, the transitions between states are not independent of each other. For instance, it has been postulated that the rate of inactivation depends on the number of open subunits and is much faster than in the standard Hodgkin–Huxley model (so-called *coupled models*; Armstrong and Bezanilla, 1977; Aldrich, Corey, and Stevens, 1983). A great deal of ingenuity continues to be spent deciphering the correct kinetic gating scheme with the help of highly refined measuring techniques. It remains an open question whether working out all the details of the underlying microscopic transitions will lead to a description of the ionic current at the macroscopic level substantially different from that in use today. Furthermore, as we will illustrate now, the large number of channels underlying most signaling in neurons allows us to average over individual stochastic channels and to only consider deterministic ionic currents.

## 8.3 From Stochastic Channels to Deterministic Currents

In Chap. 6 we learned how Hodgkin and Huxley successfully described the dynamics of the membrane voltage in terms of deterministic and graded ionic currents. Yet as detailed above,

we now know this to be caused by the current through stochastic all-or-none molecular pores. Undoubtedly, the macroscopic current is constituted by the summation of the microscopic currents sweeping through many, many channels. But what is their exact relationship? Figure 8.6 expresses the general idea: although the precise time each channel switches into its open state is a random occurrence, the average duration of channel opening has a well-described temporal onset, depending systematically on the membrane voltage. On each of the 10 trials in Fig. 8.6, the exact sequence of openings and closings of a single delayed-rectifier potassium channel differs, yet averaging over a sufficient number of trials leads to the smoothly varying current expected from the continuous Hodgkin–Huxley formalism. Indeed, since $h_\infty$ is close to 1 and $m_\infty$ is close to 0 at $-80$ mV (absolute potential; Fig. 6.4), the time course of Fig. 8.6B can be approximated by $(1 - e^{-t/\tau_m})^3 e^{-t/\tau_h}$.

A number of researchers have explored the relationship between microscopic channels and macroscopic currents (Verveen and Derksen, 1968; Lecar and Nossal, 1971a,b; Skaugen and Walloe, 1979; Skaugen, 1980a, b; Clay and DeFelice, 1983; DeFelice and Clay, 1983; Strassberg and DeFelice, 1993; Fox and Lu, 1994; Chow and White, 1996). Let us delve into this topic in a bit more detail.

### 8.3.1 Probabilistic Interpretation

Let us go back to the idea expressed in the $m^3h$ formalism of Hodgkin and Huxley. Ions are only free to drift down the potential gradient of the channel if all four gating particles are

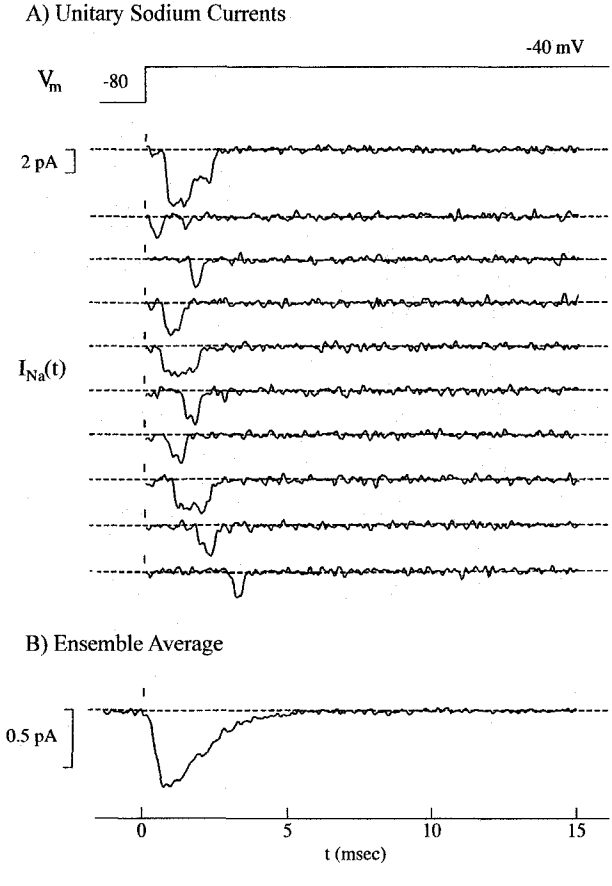


**Fig. 8.6 Stochastic Openings of Individual Sodium Channels (A)** Random opening and closing of a handful of fast sodium channels in a mouse muscle cell. The membrane potential was stepped from $-80$ to $-40$ mV; the first trial reveals the simultaneous opening of two $Na^+$ channels, while on all other trials, only a single channel was open. **(B)** Averaging over 352 such trials leads to a smoothly varying current in accordance with the $m^3h$ model of Hodgkin and Huxley. Experiment carried out at 15° C. Reprinted by permission from Patlak and Ortiz (1986).

in their open position. Let $m(t)$ be the fraction of activation particles in their open position and $\beta_m(V_m)$ the rate at which transitions occur from open to closed. In the case of the Hodgkin-Huxley model (Eq. 6.17), each 18-mV depolarization increases this rate $e$-fold. In the absence of any new open states being created, the fraction of open states must decay according to

$$\frac{dm(t)}{dt} = -\beta_m(V_m)m(t)\,. \tag{8.5}$$

If at the beginning of the experiment at $t = 0$, the fraction of particles in their open position was $m_0$, the temporal evolution of $m$ is given by

$$m(t) = m_0 e^{-\beta_m(V_m)t}\,. \tag{8.6}$$

Since we assume that the gating particles have no memory, in other words, that the probability of a given particle to change its state does not depend on its previous history (Markovian property), we can express the probability that a single particle will remain in its open position after an observation period $T$ as

$$m(T) = e^{-\beta_m(V_m)T}\,. \tag{8.7}$$

If the $m$ variable is in its closed position it can switch into its open state at the voltage-dependent rate $\alpha_m(V_m)$. The total change in the fraction of particles open is the difference between the fraction of closed particles making the transition into open states and the fraction of open states decaying away into closed states,

$$\frac{dm(t)}{dt} = \alpha_m(V_m)(1 - m(t)) - \beta_m(V_m)m(t)\,. \tag{8.8}$$

Note that this is the equation we encountered in Chap. 6 in the context of the deterministic and macroscopic Hodgkin–Huxley formalism, while here we interpret $m(t)$ in a probabilistic manner.

Let us apply this interpretation to the fast sodium channels of the squid giant axon. Adopting the simplest kinetic scheme illustrated in Fig. 8.5, we need to compute the probabilities for each sodium channel to be in one of its eight distinct states. For instance, the probability of the $m_2h_1$ state (Fig. 8.5; two activation particles and the inactivation particle all open) is given by the product (since all four particles are assumed to act independently) of the probability of finding two open activation particles ($m^2$), one closed particle ($1 - m$) and one open inactivating particle ($h$). Because any two of the three $m$ particles can be open, the final probability for this state is

$$p_1 = 3\left(\frac{\alpha_m(V_0)}{\alpha_m(V_0) + \beta_m(V_0)}\right)^2\left(1 - \frac{\alpha_m(V_0)}{\alpha_m(V_0) + \beta_m(V_0)}\right)\frac{\alpha_h(V_0)}{\alpha_h(V_0) + \beta_h(V_0)} \tag{8.9}$$

where $V_0$ is the voltage at rest. Similar expressions can be derived for all other seven states. In a Monte-Carlo computer simulation of the probabilistic openings and closings of single channels (as first carried out by Skaugen and Walloe, 1979, and Skaugen, 1980a,b), the actual initial state is computed by assigning each of the probabilities for the eight states a portion of the real line between 0 and 1. The length of this partitioning is given by the associated probability (with the sum of all probabilities equal to 1, of course) and by generating a random number $r_1$ (drawn from a uniform probability distribution between 0 and 1). The part of the line on which $r_1$ falls is the initial state.

Assume now that the membrane potential changes instantaneously from $V_0$ to $V_1$. How long will the channel remain in its initial state? The probability that the channel remains in this state after a period $T$ is

$$p_2 = e^{-(\alpha_m(V_1)+\alpha_h(V_1)+2\beta_m(V_1))T} . \tag{8.10}$$

The three constants in the exponential account for the fact that the third subunit could open (with rate $\alpha_m$), or either one of the two subunits could close again ($2\beta_m$), or the channel could inactivate ($\alpha_h$). To determine the actual lifetime, another random number $r_2$ is generated; the duration of state $m_2h_1$ is then $-(\alpha_m + \alpha_h + 2\beta_m)^{-1}\ln(r_2)$. The probability for the channel to make a transition from $m_2h_1$ to the state where all four subunits are in their open state and the channel conducts (state $m_3h_1$) is given by

$$p_3 = \frac{\alpha_m(V_1)}{\alpha_m(V_1) + \alpha_h(V_1) + 2\beta_m(V_1)} . \tag{8.11}$$

Likewise, the probability for the channel to switch from $m_2h_1$ into $m_2h_0$ is

$$p_4 = \frac{\alpha_h(V_1)}{\alpha_m(V_1) + \alpha_h(V_1) + 2\beta_m(V_1)} \tag{8.12}$$

and from $m_2h_1$ into $m_1h_1$ it is

$$p_5 = \frac{2\beta_m(V_1)}{\alpha_m(V_1) + \alpha_h(V_1) + 2\beta_m(V_1)} . \tag{8.13}$$

Partitioning the unit line into three intervals, $r_3$ is generated to decide into which state the channel has switched: if $0 < r_3 < p_3$, the open state $m_3h_1$ is chosen; if $p_3 < r_3 < p_3 + p_4$, it will be $m_2h_0$, and if $p_3 + p_4 < r_3 \leq 1$, the state $m_1h_1$ is chosen. In this manner, the life history of one particular sodium channel is simulated as the membrane is voltage-clamped (Fig. 8.7). A patch of membrane with more than one channel, where the channels are assumed to act independenty—no substantial evidence for coupling among neighboring channels has emerged—can be simulated with a more efficient procedure that keeps track of what fraction of the population is in what state (Skaugen and Walloe, 1979; Chow and White, 1996).

As witnessed by the bottom trace in Fig. 8.7, the changing conductance associated with a handful of opening and closing channels can be quite different from that of the macroscopic conductance expected by the continuous Hodgkin–Huxley equation. Yet for 600 channels, the behavior approximates that of the continuous deterministic $m^3(t)h(t)$ formulation. This is not surprising, since the central limit theorem tells us that the standard deviation of the mean of a population of $n$ independent variables increases like $\sqrt{n}$ as $n \to \infty$. Thus, the relative deviation from the mean decreases as $1/\sqrt{n}$ for large values of $n$. For 600 sodium channels, corresponding to a few square micrometer of squid membrane, the total conductance differs little from that obtained by the continuous $m^3h$ formulation. Suitably normalized, this is also the conductance obtained when experimentally averaging over hundreds of single-channel openings, as shown empirically in Fig. 8.6B.

A similar Monte-Carlo procedure can be used to calculate the behavior of a piece of squid axon membrane in the presence of a constant stimulus current (Strassberg and DeFelice, 1993). Here, the potassium channels are modeled using the simplest possible linear and noncooperative kinetic scheme with five states (four closed and one open) with the appropriate values of $\alpha_n(V_m)$ and $\beta_n(V_m)$ (with all rate constants as specified in Chap. 6). This patch of membrane is assumed to be studded with a constant density of channels (18

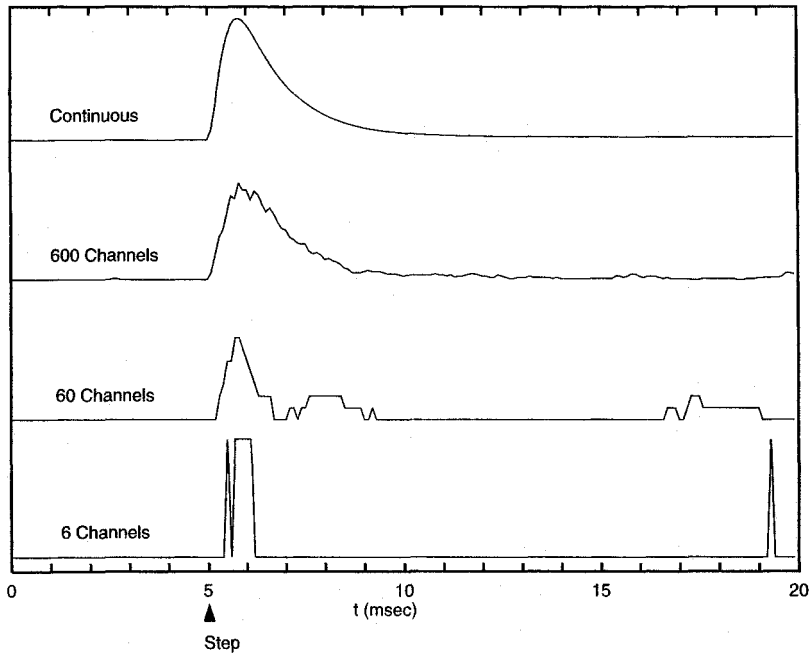


**Fig. 8.7 Simulated Life History of Individual Sodium Channels** The membrane potential in a simulated membrane patch containing a variable number of $Na^+$ channels was stepped from $V_0 = 0$ to $V_1 = 50$ mV at 5 msec (arrow). The normalized conductance associated with the eight-state Markov model shown in Fig. 8.5 was evaluated numerically for several trial runs (see Strassberg and DeFelice, 1993). As the number of channels is increased from 6 to 600, the graded and deterministic nature of the (normalized) sodium conductance emerges from the binary and stochastic single-channel behavior. The top trace shows the conductance computed using the continuous time-course (approximating $(1 - e^{-t/\tau_m})^3 e^{-t/\tau_h}$) formalism of Hodgkin and Huxley (1952). This figure should be compared against the experimentally recorded sodium current through a few channels in Fig. 8.6B. Reprinted in modified form by permission from Strassberg and DeFelice (1993).

potassium and 60 sodium channels per square micrometer) each characterized by its own state. As the size of the patch is increased from 1 to $10^4$ $\mu m^2$ (always assuming that all channels see the same membrane potential) in the presence of a constant injected current density (to normalize for the membrane area) a steady progression from random openings to a highly regular train of action potentials can be observed (Strassberg and DeFelice, 1993). For patches containing on the order of 1000 binary channels, repetitive spikes with approximately the same firing frequency (90 $\pm$ 10 Hz) as in the continuous Hodgkin–Huxley model occur (top trace in Fig. 8.8).

We saw in Fig. 6.10 how adding noise to the input current linearized the abrupt discharge curve associated with the space-clamped Hodgkin–Huxley system. A similar linear behavior has been obtained in computer simulations of the complete $f$–$I$ curve in the presence of 1000 and fewer discrete $Na^+$ channels (Skaugen and Walloe, 1979). It is only when increasing the number of $Na^+$ channels to 10,000 (while keeping $\overline{G}_{Na}$ constant) that the $f$–$I$ curve with the sudden onset of the firing characteristic of the deterministic Hodgkin–Huxley equations is recovered.

The simulations discussed here were carried out at $V_{rest}$. At more depolarized potentials the amplitudes of the channel fluctuations are larger. Indeed, it is plausible to imagine a scenario where an extended and deterministic input hovering just around firing threshold

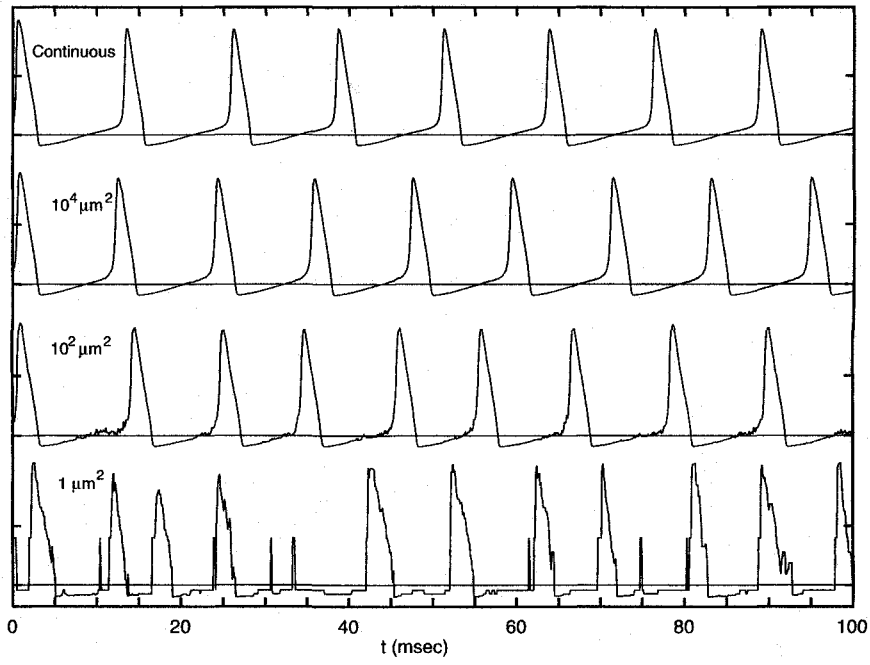


**Fig. 8.8 Action Potentials and Single Channels** Computed membrane potential (relative to $V_{rest}$ indicated by horizontal lines) in different size patches of squid axon membrane populated by a constant density of $Na^+$ and $K^+$ channels. The space-clamped membrane is responding to a current injection of 100 pA/$\mu m^2$. The transitions of each all-or-none channel are described by its own probabilistic Markov model (the eight-state model in Fig. 8.5 for the $Na^+$ channel and the simplest possible five-state linear model for the $K^+$ channel). For patches containing less than 100 channels (bottom trace), firing can be quite irregular. For patches containing dozens or fewer channels it becomes impossible to define action potentials unambiguously, since the opening of one or two channels can rapidly depolarize the membrane (not shown). As the membrane potential acts on 1000 or more binary and stochastic channels, the response becomes quite predictable, and merges into the behavior expected by numerical integration of the Hodgkin–Huxley equations for continuous and deterministic currents (top trace). The density is set to 60 $Na^+$ channels and 18 $K^+$ channels per square micrometer, each with a single channel conductance $\gamma$ of 20 pS. All other values are as specified in the standard Hodgkin–Huxley model. Reprinted in modified form by permission from Strassberg and DeFelice (1993).

causes stochastic spiking by virtue of the fact that even in a spatially extended system, fluctuations in a small number of channels are enough to exceed $V_{th}$ and initiate firing. Indeed, pyramidal cells responding to just suprathreshold, maintained current injections are known to show much more jitter in their exact timing compared to a temporally modulated current input (Mainen and Sejnowski, 1995). As sustained inputs are unlikely to occur under ecological conditions, it remains unclear to what extent the stochastic nature of ionic channels influences computations performed on physiological input.

For simulated squid axon patches of less than 1 $\mu m^2$, the opening of any one channel has an appreciable effect on the membrane potential. The all-or-none behavior of the action potential is less and less evident in these cases, since the simultaneous opening of a few channels depolarizes the membrane significantly. Given this variability in the amplitude of the membrane response, it is difficult to define a firing frequency for a very small number of channels.

We should emphasize here the obvious, namely, that individual channels do not show any threshold behavior. They do not change their configuration abruptly at some fixed voltage level. Rather, the probability of opening increases continuously with voltage. The macroscopically observed voltage (or current) threshold occurs when the sum of all inward currents through the $Na^+$ channels just about exceeds the sum of the outward currents generated by the potassium and leak conductances and by the local circuit current.

### 8.3.2 Spontaneous Action Potentials

Much more tantalizing behavior can be seen in the absence of any direct stimulus. Figure 8.9 illustrates the flat voltage trajectory associated with the continuous Hodgkin–Huxley equations when no external current is supplied. This stationary behavior also occurs for

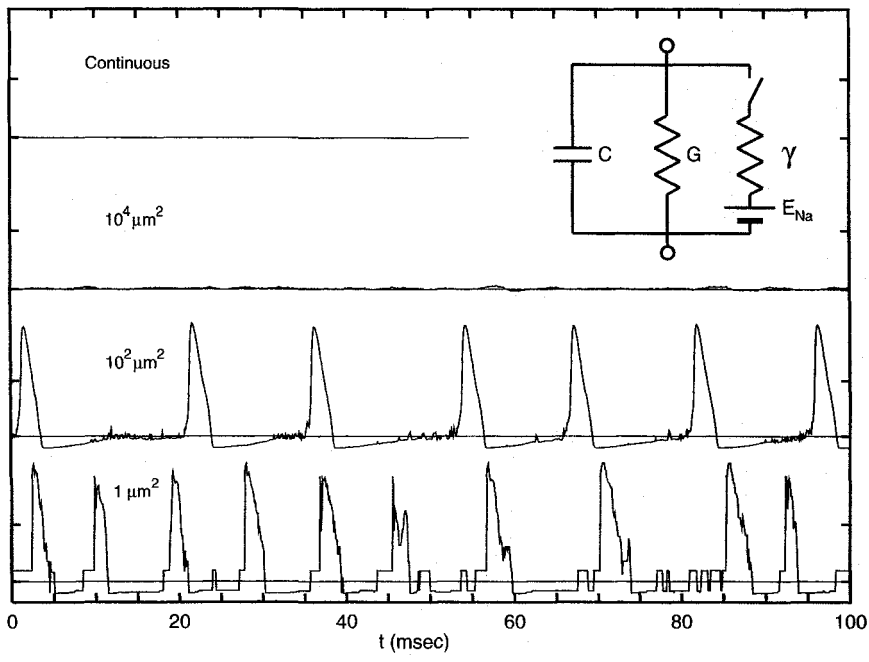


**Fig. 8.9 Spontaneous Action Potentials** The same model as is Fig. 8.8 is rerun, but now in the absence of *any* current stimulus. The bottom three traces show Monte-Carlo sample trials for axonal membrane patches of different surface areas $A$ populated with a constant density of $Na^+$ and $K^+$ channels (60 and 18 channels per square micrometer, respectively). Because the opening of a single sodium channel (of conductance $\gamma$) can give rise to a very large depolarization, the spontaneous openings of two sodium channels is enough to trigger the opening of the remaining sodium channels and the membrane generates a spike. These spikes are Poisson distributed (once a refractory period has been accounted for; Chow and White, 1996). The top trace shows the solution of the continuous and deterministic Hodgkin–Huxley equation: $V$ in the absence of a current input remains flat. The circuit inset provides the basic intuition why a single channel, in the presence of a small leak conductance $G$, can cause a large membrane depolarization. These simulations predict that in high-impedance systems with an active membrane, spontaneous spiking can be observed under certain conditions in the absence of any synaptic input. The membrane leak conductance $G$ for these three conditions corresponds to 3 pS, 300 pS, and 30 nS, as compared to a single-channel conductance of $\gamma = 20$ pS for both channel types. For more details see legend to Fig. 8.8. Reprinted in modified form by permission from Strassberg and DeFelice (1993).

simulations with several hundred thousand discrete probabilistic ionic channels (third trace from the bottom in Fig. 8.9). As the number of channels is reduced—by reducing the size of the space-clamped patch—a much more interesting behavior emerges: the axonal membrane "spontaneously" generates a train of remarkably regular action potentials.

What causes microscopic events, such as the openings of a few channels, to be so drastically amplified that they can lead to observable macroscopic phenomena? Upon inspection of the $V(t)$ trace for the smallest 1-$\mu$m$^2$ patch at the bottom of Fig. 8.9, we see many binary transitions from a value close to $E_K$ to a value a few millivolts above $V_{rest}$. These events are caused by the abrupt opening of single sodium channels. That one ionic channel can have this large effect can be understood in terms of a very simple circuit (inset in Fig. 8.9). We assume the membrane to be at rest, with a steady-state membrane leak conductance $G = AG_m$, where $A$ is the surface area of the patch and $G_m = 3$ pS/$\mu$m$^2$. Each channel opening contributes $\gamma = 20$ pS toward the total conductance, an amount independent of the surface area. The voltage trajectory following the opening of a single channel is given by

$$V(t) = \Delta V(1 - e^{-t/\tau}) \tag{8.14}$$

with $\Delta V = E_{Na}/(1 + AG_m/\gamma)$ and $\tau = AC_m/(AG_m + \gamma)$. For this simple model, $\Delta V$ in response to a single sodium channel opening is 100 mV. However, $V(t)$ in the lower trace in Fig. 8.9 hovers just above $E_K$, due to a few open potassium channels. They add enough background conductance for $\Delta V$ to be on the order of 20 mV, with the membrane potential reaching its equilibrium within a fraction of a millisecond. When two sodium channels (out of the 60 present in the 1-$\mu$m$^2$-large patch) open coincidentally, they rapidly depolarize the membrane beyond $V_{th}$ associated with the deterministic equations, thereby initiating an action potential.

The fact that the random opening of channels can induce "spontaneous" spikes is ultimately caused by the fact that while the leak conductance (and the membrane capacitance) is assumed to scale with the membrane area $A$, the channel conductance is independent of $A$. The probability that two out of 60 independently acting sodium channels are open is so high, even at $E_K$, that the membrane is either always refractory or spiking, leading to an average firing frequency of around 90 Hz. And all of this in the absence of any synaptic or current input. For larger values of $A$, the membrane depolarization produced by the simultaneous opening of a small number of channels becomes so small that the membrane potential effectively remains always around zero (third voltage trace in Fig. 8.9).

In an elegant study demonstrating how concepts from physics can be applied to neurobiological problems, Chow and White (1996) derive an analytical expression for the probability of spontaneous spiking in analogy to the classical problem of determining the probability that a particle in a double-well potential makes the transition from one well to the other. Under the assumption that sodium activation occurs at a much faster time scale than changes in $V$, $n$, or $h$, they incorporate fluctuations in $m$ into a stochastic conductance term that is added to the conventional deterministic $g_{Na}$ term. Chow and White find that the probability of spontaneous firing decays exponentially as the area of the membrane patch increases. Furthermore, the interspike intervals are exponentially distributed once the refractory period is accounted for (Chap. 15). In other words, the spontaneous spikes are Poisson distributed.

Under what circumstances could the random opening of one or a few ionic channels cause such spontaneous action potentials to occur? From an electrical point of view, this

requires a small input conductance (on the order of the single channel conductance or less) as well as a low membrane capacitance. Assuming a relatively conservative value of the membrane resistance of $R_m = 30{,}000\ \Omega{\cdot}cm^2$, implies that the entire leak conductance of a spherical 10-$\mu$m-diameter cell is about five times the open-channel conductance of a single sodium channel.

The occurrence of action potentials following the opening of a single ionic channel in cells with very high input resistances (tens of gigaohms) has been experimentally observed in chromaffin cells of the adrenal medulla (Fenwick, Marty, and Neher, 1982), rat olfactory receptor neurons (Lynch and Barry, 1989), and in hippocampal cultured neurons (Johansson and Arhem, 1994). Whether or not the opening of these channels is truly spontaneous, that is, due to thermal fluctuation in the configuration of the channel protein, or triggered by some factor in the extra- or intracellular milieu is very difficult to establish experimentally. Similar phenomena might well occur in thin spines, distal dendrites, or even the cell body of small interneurons, in particular if shielded by membrane invaginations or the cellular nucleus. Does the nervous system exploit such local sources of microscopic noise for its own, functional purposes?

## 8.4 Recapitulation

Underlying the entire gamut of electrochemical events in the nervous system are proteins inserted into the bilipid membrane, so-called ionic channels, which allow specific ions passage across the bilipid membrane. Given their small electrical conductance (between 5 and 200 pS), it required the development of the giga-seal technique by Neher and Sakmann to readily observe their behavior. From a functional point of view, the key properties of channels are that they possess one or a very small number of open, conductive states and that the transitions among closed, open, and inactivated states are governed in a probabilistic manner by the amplitude of the applied membrane potential (for voltage-dependent channels) or the presence of various agonists (for ligand-gated channels).

A very large effort in the field is directed toward identifying and characterizing the molecular sequence of these channels and in relating specific structural features of the channel protein to its voltage and ionic selectivity and, ultimately, to its function. Such a detailed molecular understanding goes hand in hand with the construction of ever more complex kinetic models, describing the transitions of a single channel among a large number of internal states in terms of probabilistic Markov models.

Numerical studies have related the microscopic, stochastic chatter of individual ionic channels opening and closing to the observance of macroscopic currents changing in a highly deterministic and graded manner. A membrane at rest and studded with a few thousand discrete channels behaves in general little different from the deterministic Hodgkin–Huxley equations. Deviations are only expected to occur when the membrane potential is close to threshold or when the channels are embedded into a small patch of neuronal membrane with a low leak conductance. In the latter case, the single-channel conductance can have the same magnitude as the passive leak conductance, and the opening of one or a few channels can depolarize the membrane beyond $V_{th}$. The resultant spikes are Poisson distributed. In other words, the microscopic behavior of individual molecules is amplified and causes a macroscopic event, an action potential. Such a mechanism, known to occur in certain experimental preparations, could be of functional relevance in very small

cells or in electrically decoupled, distal parts of the dendritic tree as a "random event" generator.

In the remainder of this book we will typically deal with large enough membrane areas—and therefore channel numbers—that we are usually justified in treating electrical events in terms of deterministic, continuous currents, rather than in terms of probabilistic, all-or-none ionic channels.